Available online at www.sciencedirect.com

ScienceDirect

Energy Procedia 161 (2019) 472–479

Energy Procedia

www.elsevier.com/locate/procedia

2nd International Conference on Sustainable Energy and Resource Use in Food Chains, ICSEF 2018, 17-19 October 2019, Paphos, Cyprus

Numerical modelling and performance maps of a printed circuit heat exchanger for use as recuperator in supercritical CO_2 power cycles

Matteo Marchionni, Lei Chai, Giuseppe Bianchi*, Savvas A.Tassou

Brunel University London, Institute of Energy Futures, Centre for Sustainable Energy use in Food chains (CSEF) Uxbridge, UB8 3PH, United Kingdom

Abstract

In heat to power systems with CO_2 as working fluid in the supercritical state (sCO_2), heat exchangers account for nearly 80% of the capital expenditure. Therefore, improved design, materials and manufacturing methodologies are required to enable the economic feasibility of the sCO_2 technology. In this study, a comparison of different modelling methodologies for Printed Circuit Heat Exchangers (PCHE) is proposed to identify strengths and weaknesses of both the approaches. The elementary heat transfer unit of a PCHE recuperator for sCO_2 applications is firstly modelled using 1D and 3D CFD methodologies respectively; implemented in GT-SUITE and ANSYS FLUENT software. After the comparison in terms of heat transfer performance and pressure drops, the 1D approach is used to model a 630kW PCHE recuperator. The PCHE model calibration on the design point, followed by its validation against off-design operating points provided by the manufacturer, eventually enabled to broaden the simulation spectrum and retrieve performance maps of the device. The CFD models comparison shows a good agreement between temperature profiles. However, the local heat transfer coefficient, modelled in the 1D approach through the Dittus-Boelter correlation, experiences a +10% offset on the hot side and a -20% on the cold one with respect to the 3D CFD calculations. Besides, the performance maps of the full scale PCHE recuperator show that the maximum temperature of the hot stream impose a greater influence than the maximum pressure of the cold one in terms of overall heat transfer coefficient. Nonetheless, both these operating parameters contribute to affect the heat exchanger effectiveness.

Selection and peer-review under responsibility of the 2nd International Conference on Sustainable Energy and Resource Use in Food Chains, ICSEF2018

Keywords: PCHE recuperator; 1D CFD modelling; PCHE optimisation; sCO2 power cycles;

* Corresponding author. Tel.: +44-1895-267707; fax: +44-1895-269777.
E-mail address: giuseppe.bianchi@brunel.ac.uk

Selection and peer-review under responsibility of the 2nd International Conference on Sustainable Energy and Resource Use in Food Chains, ICSEF2018.
10.1016/j.egypro.2019.02.068

1. Introduction

Power generation systems based on Joule-Brayton cycles and with supercritical CO_2 (sCO_2) as working fluid are a promising technology for nuclear, concentrated solar as well as high-grade heat to power conversion [1,2]. Their underpinning potential is indeed the superior performance at more contained investment costs. Nevertheless, the technology readiness level of sCO_2 power systems is still limited, and more research is demanded to address some key technological challenges. Among them, the development of reliable and cost-effective heat exchangers is of paramount importance since they not only represent one of the main technological barrier to enhance the cycle efficiency and net power output but they also account for almost the 80% of the capital expenditure for a new plant [3]. In fact, with reference to a simple regenerated sCO_2 Joule-Brayton cycle layout, at least three heat exchangers are needed, i.e. gas cooler, recuperator and gas heater. Moreover, these equipment operate at high pressures (from 75 bar to 250 bar) and with severe thermal duties (up to 1 MW/m^2) [3].

If the sCO_2 heater is the most challenging piece of equipment with regards to materials and thermo-structural stresses, the recuperator performance has a significant impact on the cycle efficiency [4]. In this area, Printed Circuit Heat Exchangers (PCHEs) are an established and mature technology. They are able to not only withstand thermal stresses and operating pressures up to 1000 bar, but also provide high heat transfer rates while maintaining a high compactness (80-200 kg/MW) [5].

Several works have been carried out to analyse and optimise the thermo-hydraulic performance of PCHEs and to study the local heat transfer phenomena occurring in the channels. Among them, numerical investigations of a conventional PCHE were performed through a three dimensional (3D) Computational Fluid Dynamic (CFD) approach and the results compared with experimental data [6]. New design concepts which investigated the heat transfer enhancement due to the adoptions of fins and their shape optimisation were presented in references [7,8]. Experimental assessments were further carried out in references [9–11] and mainly focused on the characterisation of the thermo-hydraulic behavior of conventional zig zag PCHE.

The afore mentioned literature studies were oriented to the PCHE optimisation from a technological viewpoint. However, from a plant perspective, the heat exchangers operation triggers a series of changes in the other components (e.g. turbomachinery) which ultimately affect the performance of the whole sCO_2 system. These phenomena are even more severe at off-design conditions and cannot be investigated with high fidelity models due to complexity and computational cost concerns. To address this research need, in this paper a one-dimensional (1D) model of the elementary unit of a PCHE is presented and compared to 3D CFD calculations. After the validation of the modelling approach, a 1D model for a 631kW PCHE used as recuperator in a sCO_2 system is presented and validated with respect to off-design performance with the figures provided by the manufacturer. Finally, the performance maps of the printed circuit recuperator in terms of overall heat transfer coefficient, effectiveness and the total pressure drop of the heat exchanger are shown as a function of the maximum cycle pressure, temperature and CO_2 mass flow rate.

2. Methodology

The test case used for comparison between the numerical 3D and 1D CFD methodologies is the elementary heat transfer unit of a PCHE, i.e. two straight channels in cross-flow and with half-semicircular cross-section. Figure 1a shows the 3D geometry while Fig 1b the equivalent 1D network. The hot stream is represented in red while the cold one in blue. Geometrical features and materials are summarised in Table 1. In both cases, the thermophysical properties of CO_2 have been calculated with reference to the NIST Refprop database through a dynamic-link library (DLL) [12].

In the 3D model, due to the periodic structure of the PCHE, periodic boundary conditions are imposed at the top and bottom surfaces, while symmetric boundary conditions are set on the sides, as shown in Fig 1a. The conservation equations for both streams are solved using the CFD solver of ANSYS FLUENT 17.0. In particular, the SIMPLEC algorithm is used to solve the coupling between pressure and velocity while the second order upwind is applied to discretise the convection terms. The flow turbulence has been taken in account by adopting the standard k-ε model [13]. Buoyancy and entrance effects are also considered.

In the 1D model, developed in GT-SUITE™, the channels have been discretised along the flow direction as per Fig. 1b. In particular, for each segment, the semicircular cross-section has been specified by setting as input the cross-

sectional area, the wetted parameter and the hydraulic diameter. Each flow channel block is connected through a convective connection (grey circle denoted by the letter "h" in Fig. 1b) to a discretised metallic mass, which represents the metal portion of the elementary PCHE unit delimited by the two sub-volumes of the channels (the grey square with a red point in the center, Fig. 1b). This metallic mass represents the discretised thermal inertia of the heat exchanger and it also specifies the material properties, such as the thermal conductivity and the density as a function of the material temperature. The discretised thermal masses are all inter-connected by a conductive connection. To compute the heat transfer coefficient along the channels, the Dittus-Boelter correlation has been considered while the calculation of the pressure drops is based on the Colebrook equation; a more detailed description of the modelling procedure can be found in reference [14].

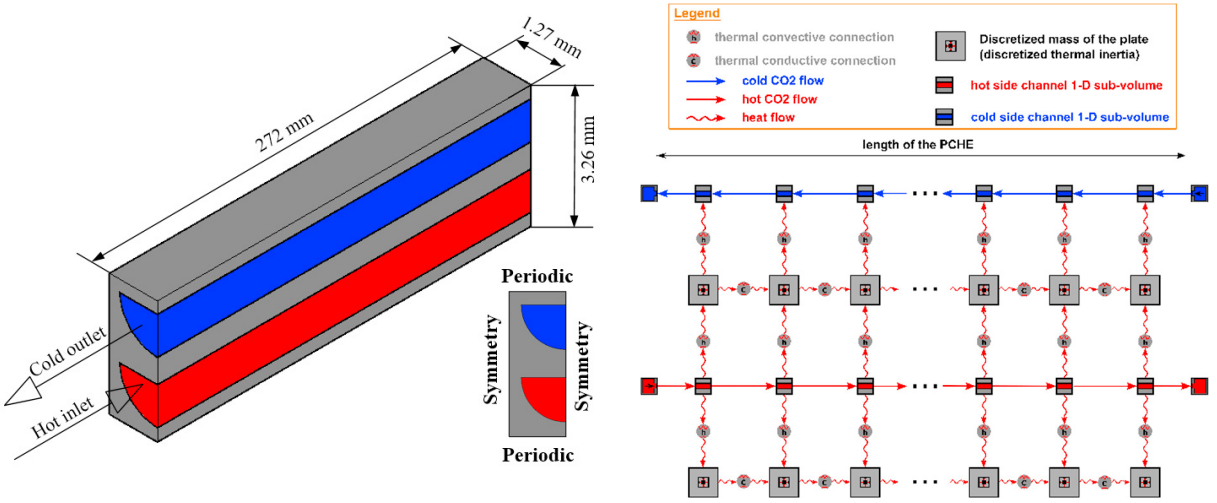

Fig. 1. Computational domains for the elementaty heat transfer unit of a PCHE: 3D (a) and 1D (b) approaches

Table 1. Geometrical features and materials of the test case in Fig. 1

Wetted perimeter [mm]	5.14
Hydraulic diameter [mm]	1.22
Cross-sectional area [mm^2]	1.57
Length [mm]	272.00
Plate thickness [mm]	1.63
Surface roughness	Neglected
Material	Stainless steel 316L

Table 2. Simulation setups

Boundary conditions	Cold side	Hot side
Mass flux [kg/m^2]	509.3	
Inlet temperature [°C]	100	400
Outlet pressure [bar]	150	75
	1D	3D
Spatial discretization [mm]	6.8	<0.05
Computational time	5 seconds	1 day

The initial conditions are summarised in Table 2 and expressed in terms of inlet temperature and pressure of the two CO_2 streams; since the simulations refer to a PCHE recuperator, the mass flux is the same on both channels.

Both the simulations were run as serial cases: the 3D one using an Intel Xeon E5-2670 CPU at 2.6 GHz required 2.9 GB of RAM; the 1D one using an Intel Core i7-6700 CPU at 3.4 GHz required 0.4 GB of RAM. Differences in terms of computational time and resources are not only due to the larger computational domain but also to the DLL interface with the Refprop database. In fact, 3D simulations would last 4 hours assuming constant CO_2 properties.

3. Results and discussion

This section firstly reports the comparison of the 1D model results against the 3D benchmark. Afterwards, the 1D methodology is used to model a 631kW PCHE recuperator. The model is firstly validated against design and off-

design performance provided by the manufacturer and ultimately exploited to generate performance maps of the device.

3.1. CFD models comparison

With reference to the modelling methodologies and setups reported in Section 2, Figure 2 summarises the comparison between 1D and 3D CFD results. In particular, Figure 2.a shows the local heat transfer coefficient between the cold and hot sCO2 flow and the PCHE channel wall respectively, while Figure 2.b and 2.c compare the temperatures and the pressure drops as a function of the duct length.

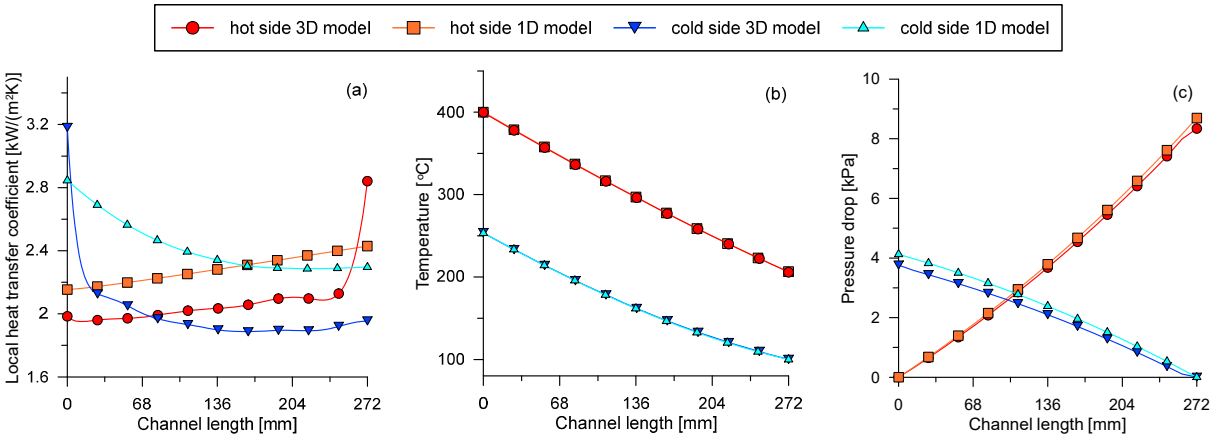

Fig. 2. Comparison of the results obtained by the 1D and 3D CFD model simulations:
(a) local heat transfer coefficient, (b) hot and cold flow temperatures, (c) pressure drops

From Fig 2b and 2c, it is possible to notice that the temperatures and the pressure drops along the channel obtained by the 1D simulation resemble the data obtained by the 3D one; this validates the 1D modelling procedure.

Nonetheless, Fig 2a shows that, even if the trends coincide, the local heat transfer coefficients slightly mismatch. In fact, if the cross-section in the middle of the channel is considered (meaning at distance of 136 mm from the channel entry cross-section), the local heat transfer coefficient of the cold side in the 3D model is equal to 1.90 kW/(m^{2}K), while the 1D one predicts a value of 2.34 kW/(m^{2}K), showing an error of 23.4%. Also the local heat transfer of the hot side is over predicted, since for the same cross section, the value calculated by the 1D model is 2.28 kW/(m^{2}K) against the 2.04 kW/(m^{2}K) computed by the 3D one, with a relative error of 12%. This prediction misalignment can be explained by considering the different calculation procedure of the local heat transfer coefficient for the two models. The 3D one in fact, computes this quantity from the solution of the velocity and thermal field for each cross section and the geometrical properties of the channel. The 1D model on the contrary, bases this calculation on the set heat transfer correlations and the thermophysical properties of the material.

An additional difference lies in the prediction of the entry effect of the two flows in the channels. Although it is taken into account in the 3D model, it is neglected by the 1D one. Indeed, it can be observed in Fig 2a that at the entry section of the cold and hot channel (0 mm and 272 mm respectively) the heat transfer coefficient computed by the full CFD model is 3.18 kW/(m^{2}K) and 2.84 kW/(m^{2}K) respectively, while the one dimensional model returns a value of 2.84 kW/(m^{2}K) and 2.43 kW/(m^{2}K). Although this last error can be neglected for design and optimisation analyses, a corrective coefficient should be used to take into account the differences in the local heat transfer predictions.

3.2. Full scale PCHE model development and calibration

After the validation of the 1D modelling procedure, this approach has been used to develop a model of a 630kW recuperator provided by a well-known manufacturer that will be used in the sCO_2 Brayton cycle test rig currently under development at Brunel University London [15]. To do so, the design point and four off-design operating

conditions of the heat exchanger have been simulated and the results compared with the data provided by the manufacturer. Table 3 and 4 summarise the specifics of the channels and PCHE respectively, while Table 5 refers to the model validation. The calibration procedure was performed on heat transfer and pressure drop multipliers such that the least square error on the five calibration points was minimised.

Table 3. PCHE channels characteristics

Channel geometry	
Wetted perimeter [mm]	5.14
Hydraulic diameter [mm]	1.22
Cross-sectional area [mm^2]	1.57
Length [mm]	1012.00
Type	Straight

Table 4. 630 kW PCHE features

PCHE properties	
Material	Stainless steel 316L
Channel surface roughness	Neglected
Channel discretization length [mm]	25.30
Number of channels per row	54
Number of rows	42

Table 5. Off-design operating condition of the 631 kW PCHE (cold side (cs) inlet pressure= 75 bar; hot side (hs) inlet pressure and temperature = 125 bar and 344.3°C)

	Design		Off-design #1		Off-design #2		Off-design #3		Off-design #4	
	1D	OEM	1D	OEM	1D	OEM	1D	OEM	1D	OEM
mass flow rate [kg/s]	2.06		1.57		2.09		2.09		2.62	
cs inlet temperature [°C]	72.9		72.9		87.5		62.0		72.9	
hs pressure drop [kPa]	127	130	78	79	146	145	121	122	199	202
hs outlet temperature [°C]	77.9	80.5	77.4	78.6	97.6	99.7	64.8	66.6	84.5	82.7
cs pressure drop [kPa]	118	120	73	74	138	139	105	106	174	184
cs outlet temperature [°C]	288	284.9	289.2	287.2	296.7	294.5	271.9	269.3	278.9	282.3
heat load [kW]	640	631	488	485	591	586	697	684	782	793

It is possible to notice from Table 5 that the 1D model is in agreement with the performance provided by the manufacturer. In particular, the pressure drop predictions match, with the highest error of 5.7% for the cold CO_2 flow in the 4th off-design case (for a working fluid mass flow rate of 2.62 kg/s, which is the 125% of the value at the design point), and an average error of 1.1% and 2.2% for the hot and the cold side respectively. The PCHE outlet temperatures and heat load predictions present also negligible deviations. In fact, the average error for the outlet temperatures of the cold and the hot side are 0.9% and 2.15% respectively, while a 1.23% average error is returned for the heat load.

3.3. PCHE performance maps

Consequently, exploiting the high simulation speed guaranteed by the 1D model, a series of sensitivity analyses have been carried out and the results reported in Figure 3. In particular, the thermal power exchanged, the overall heat transfer coefficient, the effectiveness and the sum of the pressure drops in the hot and the cold side of the PCHE are displayed as a function of the PCHE maximum pressure and temperature for a mass flow rate of 1.57 kg/s (Fig. 3a-d), 2.09 kg/s (Fig. 3e-h) and 2.62 kg/s (Fig. 3i-n).

It is possible to observe that although this change in the mass flow rate has a beneficial effect on the overall heat transfer coefficient, it negatively affects the effectiveness of the heat exchanger. In fact, for a sCO_2 mass flow of 1.57 kg/s, which corresponds to the 75% of the one at the design point, the PCHE shows a maximum effectiveness of 0.87 (Fig. 3c); while when the mass flow rate is increased to 2.62 kg/s (125% of the mass flow at the design point), the effectiveness drops down to a maximum value of 0.84 (Fig. 3m). This drop can be explained considering that when the geometry of the heat exchanger is fixed, an increase of mass flow rate not only provokes a rise of the total heat rate, but also a steeper increment in the maximum exchangeable heat rate, decreasing thus the effectiveness of the device.

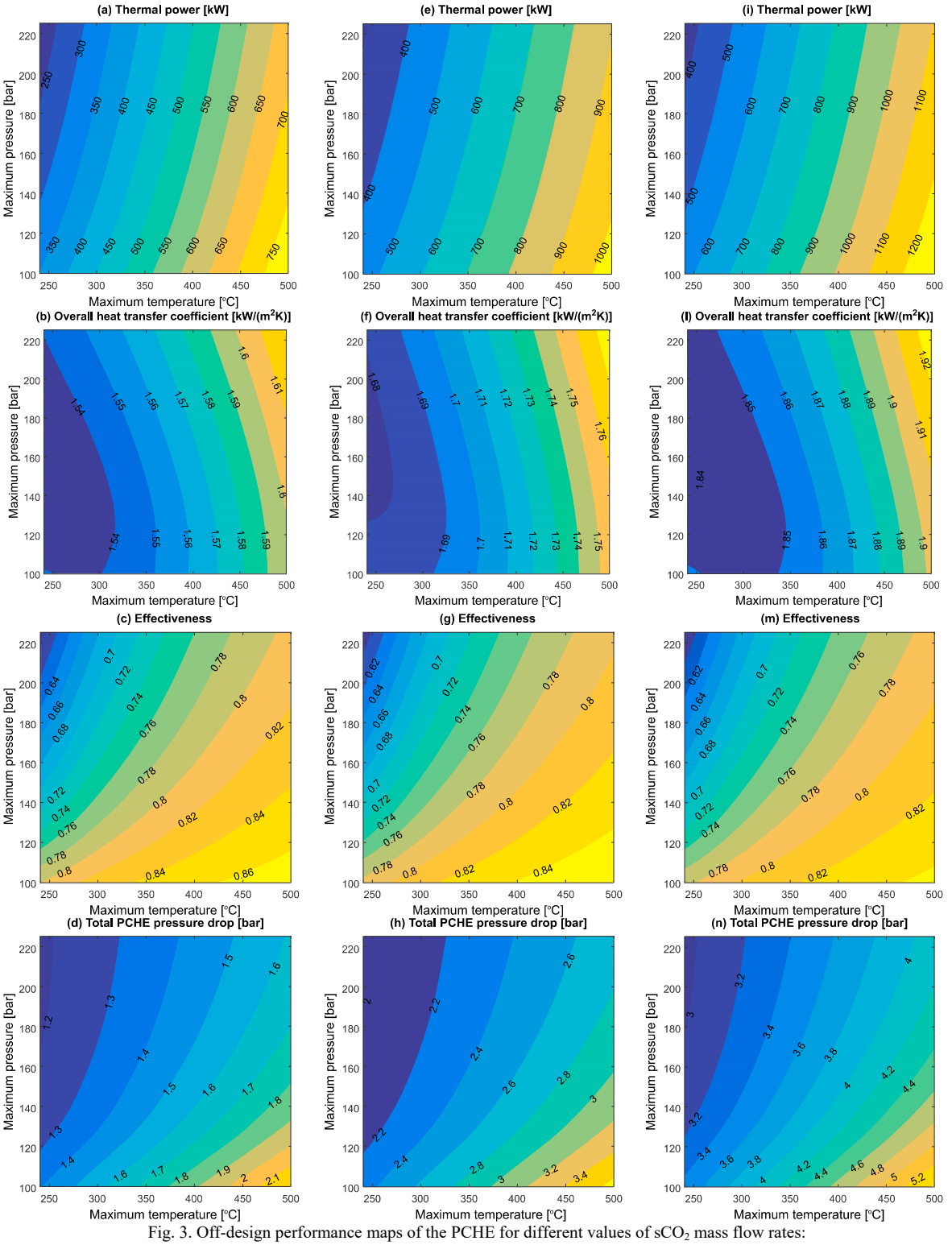

Fig. 3. Off-design performance maps of the PCHE for different values of sCO_2 mass flow rates: 1.57 kg/s (a-d), 2.09 kg/s (e-h) and 2.62 kg/s (i-n)

Also the maximum pressure of the PCHE negatively affects the effectiveness, if in fact a mass flow rate of 2.09

kg/s and a maximum temperature of 400°C is considered, an increase of pressure from 120 bar to 180 bar drops down the effectiveness from 0.82 to 0.78 (Fig. 3g). On the other hand, the same relative increase in the maximum PCHE temperature (from 300°C up to 450°C at a pressure of 120 bar) rises the effectiveness of the heat exchanger from 0.78 up to 0.83 (Fig. 3g).

The same trend can be observed for the total pressure drops in the PCHE, which decrease when the maximum pressure is increased, and increase when a rise of the maximum temperature occurs. However, in this case the influence of the pressure is more marked at high temperatures rather than at lower ones, since for a 50% of PCHE maximum pressure increment, a pressure drop decrease of 0.8 bar at 450 °C against a 0.4 bar at 300°C (Fig. 3n).

On the contrary, the overall heat transfer coefficient is enhanced from both the maximum operating pressure and temperature of the PCHE (Fig. 3b, 3f and 3l), with the maximum temperature showing a more marked effect. In fact, for a certain sCO_2 mass flow (i.e 2.62 kg/s), when the maximum temperature is increased from 300°C to 450°C at a cold side pressure of 140 bar, the overall heat transfer coefficient rises from 1.84 kW/(m^{2}K) up to 1.89 kW/(m^{2}K) (Fig. 3l). Instead, for a fixed temperature of 350°C the same relative 50% increase in pressure (from 120 bar to 180 bar), provokes a rise in the heat transfer coefficient from 1.85 kW/(m^{2}K) up to 1.86 kW/(m^{2}K).

These results should be taken into account for the selection of the recuperator in the design and optimisation stage of a sCO_2 power unit. In fact, among the main bottlenecks to enhance the efficiency of such systems are the high thermal duty at which the heat exchangers must operate and the reduction of the pressure drops along the cycle, in order not to compromise excessively the expansion ratio across the turbine, which is related to the cycle net power output. Similarly, the analysis shows that with regards to the recuperator, some trade-offs have to be addressed when the operating parameters of the cycle are selected.

In fact, even if high maximum cycle temperature is always beneficial in terms of turbine efficiency and so for the net power output, it increases the pressure drops in the PCHE and therefore erodes the expansion ratio available across the machine. In the same fashion, increasing the maximum cycle pressure leads to an augmented cycle pressure ratio and to a reduction of the pressure drops (Fig. 3.d, 3.h and 3.n) in the recuperator, but also decreases its effectiveness and thus requires a larger device to accommodate the same thermal duty, meaning higher capital expenditures.

4. Conclusions

In this work a 1D model of a PCHE has been presented. The consistency of the modelling procedure has been assessed through a comparison with numerical data obtained through 3D CFD simulations. After the validation, the 1D model has been calibrated to resemble the design and off-design operating conditions of a 630 kW PCHE supplied by a well-known manufacturer. Performance maps of the heat exchanger were obtained by varying the maximum operating pressure, temperature and CO_2 mass flow rate.

The results showed that the mass flow rate has a negative effect on the heat exchanger effectiveness, which drops from a maximum value of 0.87 for a mass flow rate of 1.57 kg/s to a value of 0.84 for a relative mass flow rate increase of 50%. The maximum cycle pressure affects negatively the effectiveness while it has a positive effect on the PCHE total pressure drop, which decreases from 0.8 bar to 0.4 bar at a temperature of 450°C and 300°C respectively for a 50% increment of the maximum operating pressure. On the contrary, a maximum temperature increase has a negative effect on the total pressure drops while it is beneficial for the overall heat transfer coefficient (which rises from 1.84 kW/(m^{2}K) to 1.89 kW/(m^{2}K) when the hot side inlet temperature increases from 300°C to 450°C).

In conclusion, the results showed that the influence of the sCO_2 cycle parameter selection on the PCHE performance must be considered. In fact, although the maximum cycle temperature and pressure positively affect the cycle efficiency and net power output, they could also increase the pressure drops across the recuperator and reduce its effectiveness, with a consequent erosion of the pressure ratio across the turbine and an increase of the heat exchanger dimensions and investment costs.

Acknowledgements

The work presented in this paper is supported by a number of funders as follows: i) The Engineering and Physical Sciences Research Council (EPSRC) of the UK under research grants EP/P004636/1 ‘Optimising Energy Management in Industry - OPTEMIN', and EP/K011820/1 (Centre for Sustainable Energy Use in Food Chains) and ii) the European Union’s Horizon 2020 research and innovation programme under grant agreement No. 680599. The Authors would

like to acknowledge the financial support received by the project funders and the industry partners. The data used in the analysis are given in the paper but if more data or information is required they can be obtained by contacting the corresponding author.

References

[1] Persichilli M, Kacludis A, Zdankiewicz E. Supercritical CO2 Power Cycle Developments and Commercialization: Why sCO2 can Displace Steam Ste. Power-Gen India & 2012.
[2] Marchionni M, Bianchi G, Tassou SA. Techno-economic assessment of Joule-Brayton cycle architectures for heat to power conversion from high-grade heat sources using CO2 in the supercritical state. Energy 2018;148:1140–52. doi:10.1016/J.ENERGY.2018.02.005.
[3] Brun K, Friedman P, Dennis R. Fundamentals and applications of supercritical carbon dioxide (sCO2) based power cycles. Woodhead Publishing an imprint of Elsevier; 2017.
[4] Musgrove GO, Pierres R Le, Nash J. Heat Exchangers for Supercritical CO2 Power Cycle Applications. 4th Int Symp Supercrit CO2 Power Cycles 2014:1–61.
[5] Li Q, Flamant G, Yuan X, Neveu P, Luo L. Compact heat exchangers: A review and future applications for a new generation of high temperature solar receivers. Renew Sustain Energy Rev 2011;15:4855–75. doi:10.1016/J.RSER.2011.07.066.
[6] Kim DE, Kim MH, Cha JE, Kim SO. Numerical investigation on thermal–hydraulic performance of new printed circuit heat exchanger model. Nucl Eng Des 2008;238:3269–76. doi:10.1016/J.NUCENGDES.2008.08.002.
[7] Liu S, Huang Y, Wang J. Theoretical and numerical investigation on the fin effectiveness and the fin efficiency of printed circuit heat exchanger with straight channels. Int J Therm Sci 2018;132:558–66. doi:10.1016/J.IJTHERMALSCI.2018.06.029.
[8] Ngo TL, Kato Y, Nikitin K, Tsuzuki N. New printed circuit heat exchanger with S-shaped fins for hot water supplier. Exp Therm Fluid Sci 2006;30:811–9. doi:10.1016/J.EXPTHERMFLUSCI.2006.03.010.
[9] Ma T, Li L, Xu X-Y, Chen Y-T, Wang Q-W. Study on local thermal–hydraulic performance and optimization of zigzag-type printed circuit heat exchanger at high temperature. Energy Convers Manag 2015;104:55–66. doi:10.1016/J.ENCONMAN.2015.03.016.
[10] Li H, Zhang Y, Zhang L, Yao M, Kruizenga A, Anderson M. PDF-based modeling on the turbulent convection heat transfer of supercritical CO2 in the printed circuit heat exchangers for the supercritical CO2 Brayton cycle. Int J Heat Mass Transf 2016;98:204–18. doi:10.1016/J.IJHEATMASSTRANSFER.2016.03.001.
[11] Kwon D, Jin L, Jung W, Jeong S. Experimental investigation of heat transfer coefficient of mini-channel PCHE (printed circuit heat exchanger). Cryogenics (Guildf) 2018;92:41–9. doi:10.1016/J.CRYOGENICS.2018.03.011.
[12] Lemmon EW, Huber ML, Mclinden MO. NIST Reference Fluid Thermodynamic and Transport Properties— REFPROP User's Guide 2013.
[13] Mohammadi B, Pironneau O. Analysis of the K-epsilon turbulence model. Wiley; 1994.
[14] Marchionni M, Bianchi G, Karvountzis-Kontakiotis A, Pesiridis A, Tassou SA. Dynamic modeling and optimization of an ORC unit equipped with plate heat exchangers and turbomachines. Energy Procedia 2017;129:224–31. doi:10.1016/J.EGYPRO.2017.09.146.
[15] De Miol M, Bianchi G, Henry G, Holaind N, Tassou SA, Leroux A. Design of a single-shaft compressor, generator, turbine for small-scale supercritical CO2 systems for waste heat to power conversion applications. n.d. doi:10.17185/duepublico/46086.